Am J Transl Res 2021;13(9):9983-9992
www.ajtr.org /ISSN:1943-8141/AJTR0130172

*Original Article*

# Chest CT imaging characteristics and their evolution of 48 patients with COVID-19 in Hengyang, China

Yanfen Tang[1*], Hongwu Liao[2,7*], Qing Wu[3], Wei Li[1], Liu Peng[4], Xia Yang[3], Jinling Peng[3], Xiaoqing Tang[5], Ting Xie[6], Xuefeng Yang[3,4]

*[1]Department of Radiology, The Affiliated Nanhua Hospital, Hengyang Medical College, University of South China, Hengyang 421002, Hunan, China; [2]Institute of Clinical Research, The Affiliated Nanhua Hospital, Hengyang Medical College, University of South China, Hengyang 421002, Hunan, China; [3]Department of General Practice, The Affiliated Nanhua Hospital, Hengyang Medical College, University of South China, Hengyang 421002, Hunan, China; [4]Department of Gastroenterology, The Affiliated Nanhua Hospital, Hengyang Medical College, University of South China, Hengyang 421002, Hunan, China; [5]Institute of Clinical Medicine, The First Affiliated Hospital, Hengyang Medical College, University of South China, Hengyang 421002, Hunan, China; [6]Department of Nephrology, The Affiliated Nanhua Hospital, Hengyang Medical College, University of South China, Hengyang 421002, Hunan, China; [7]Health School of Nuclear Industry, Hengyang 421002, Hunan, China. [*]Equal contributors.*

Received January 15, 2021; Accepted May 10, 2021; Epub September 15, 2021; Published September 30, 2021

**Abstract:** The novel coronavirus 2019 (2019 nCoV), appeared in Wuhan in December 2019, can cause a novel coronavirus pneumonia (Corona Virus Disease 2019, COVID-19). COVID-19 is highly infectious and easy to infect people. The epidemic has gradually spread to all parts of the country. In order to provide a basis for clinical diagnosis, this study retrospectively analyzed the imaging characteristics, evolution and related imaging manifestations of COVID-19 patients in different stages of the disease. The results suggest that the imaging findings of 48 COVID-19 patients from Hengyang, Hunan Province are comparable in different stages of the disease. Chest CT showed no pneumonia in one mild patient. Chest CT findings of moderate type (n=38) and severe type (n=9) had comparable characteristics. The main manifestations were ground-glass opacity (GGO) (18/38, 47.37%; 1/9, 11.11%), and GGO with consolidation (16/38, 42.11%; 5/9, 55.56%), which respectively presented in bilateral lungs (34/38, 89.47%; 9/9, 100.00%), and multi-lobe distribution (involving 5 lobes) (17/38, 44.74%; 8/9, 88.89%). After treatment, 28 patients were isolated for 14 days and returned to the hospital for re-examination; among them, the pulmonary lesion was completely absorbed in 15 moderate patients, while 13 patients mainly manifested as GGO. The CT imaging findings of patients with COVID-19 can detect the lesions early, observe the scope of the lesions, evaluate the severity of the lesions, and assist the clinician in completing rapid isolation, diagnosis and treatment. At the same time, it can help to understand the performance of COVID-19 in different stages and dynamically detect changes in the patient's condition.

**Keywords:** COVID-19, SARS-CoV-2, CT scan, clinical classification, residual lesions

## Introduction

In December 2019, there have been many patients of unexplained viral pneumonia in Wuhan, and it was subsequently found to be caused by a novel coronavirus through sequencing the respiratory tract specimens [1, 2]. On February 11, 2020, the Coronavirus Research Group of the International Commission for Classification of Viruses named the novel coronavirus as SARS-Cov-2. On the same day, the World Health Organization named the disease caused by SARS-Cov-2 as "Coronavirus Disease 2019, COVID-19".

The diagnosis of COVID-19 is generally based on comprehensive judgments such as clinical manifestations, epidemiological history, imaging examinations and laboratory tests. The nucleic acid detection of 2019-nCoV is the gold standard for COVID-19. However, the current data show that the virus nucleic acid detection

has strong specificity but poor sensitivity and may generate false negatives. Some symptomatic positive patients have shown negative nucleic acid results, but the signs of infection are obvious, that is, the chest computerized tomography shows characteristic pneumonia manifestations. For asymptomatic infections and nucleic acid false-negative patients, the positive performance of chest CT has important warning signs, which highlights the importance of chest CT for accurate diagnosis of COVID-19 [3-5]. Research shows that chest CT has high sensitivity in detecting COVID-19, which is conducive to the early detection of lesions and the assessment of the nature and scope of the lesions [6]. It has been widely used in the screening, re-examination, pre-discharge evaluation and post-discharge follow-up of COVID-19 patients. It is a fast and non-invasive method that has become an important part of COVID-19 diagnosis and treatment. COVID-19 chest CT lesion manifestations and evolution are complex, similar to SARS, MERS and other viral pneumonias. The HRCT findings of COVID-19 also overlap with mycoplasma pneumonia, bacterial pneumonia and cardiogenic pulmonary edema. Thus, the differential diagnosis is difficult [7]. Therefore, how to safely and quickly complete the chest CT examination and make accurate and rapid judgments is of great significance to the diagnosis and treatment of COVID-19.

In order to improve the accuracy of early diagnosis of COVID-19, and to conduct dynamic evaluation of the patient's condition, in this study, by dynamically observing the chest CT of patients with different disease stages and clinical classifications, we summarized the imaging characteristics and performance, and speculated the development and evolution of COVID-19, so as to provide references for early clinical diagnosis and treatment of COVID-19.

## Patients and methods

### *Patients*

We retrospectively analyzed the chest CT images of 48 patients (different hospitals in Hengyang City) with COVID-19. On February 4, 2020, all patients were transferred to the Affiliated Nanhua Hospital, Hengyang Medical College, University of South China, for further treatment. The diagnostic criteria, clinical classification and discharge standard related to COVID-19 were in line with the Diagnosis and Treatment Protocol for Novel Coronavirus Pneumonia (Trial Version 7) issued by the National Health Commission [7]. The general information of the patients is shown in **Table 1**.

### *CT examinations*

Patients wore surgical masks and protective clothing during the whole examination. Technicians operated under the whole protection. Scanning parameters were tube voltage 120 kV, tube current 100-400 mA, screw pitch 1:1, scanning layer thickness 1.25 mm, and layer distance 1.25 mm. HRCT high-resolution algorithm was adopted for imaging reconstruction, with a matrix of 512 × 512. The scanning range was from the thoracic inlet to the phrenic top and the inspiratory end. The machine room was disinfected immediately after the scan was completed. Imaging analysis was performed using the WinningSoft PACS system (version TView6.1). Two senior radiologists read the film together to analyze the imaging manifestations and their dynamic changes, including the distribution, scope, type, evolution and pleural changes of pulmonary lesions.

### *Imaging evaluation*

Staging of disease: According to the onset time and course of the disease in the Guidelines for Imaging Diagnosis in Novel Coronavirus Pneumonia (2nd Edition 2020) issued by the Infectious Diseases Radiology Group of Chinese Society of Radiology, novel coronavirus pneumonia was classified into an early stage, progressive stage, peak stage and absorption stage [1]. Because some patients were first diagnosed in other hospitals, the primary chest CT results were missing. Finally, there were 28 patients at an early stage, 39 patients at a progressive stage, 41 patients at a peak stage and 47 patients at an absorption stage.

Clinical classification: The clinical classification was made according to Diagnosis and Treatment Protocol for COVID-19 (Trial Version 7) [7]. Since mild patient showed no imaging manifestations of pneumonia, the mild patient was not included in this study. The 47 COVID-19 patients included 38 of moderate type and 9 of severe type.

**Table 1.** The general information of the patients with COVID-19

| Normal information | Patients (n=48) |
|---|---|
| Gender | |
| Male | 31 (64.58%) |
| Female | 17 (35.42%) |
| Average age (years) | 44.35 ± 15.76 |
| Basic illness | |
| Coronary heart disease | 2 (4.17%) |
| Hypertension | 1 (2.08%) |
| Chronic hepatitis B | 7 (14.58%) |
| Coronary heart disease complicated with hypertension, diabetes, and cerebral infarction | 1 (2.08%) |
| Diabetes complicated with hypertension and hyperlipidemia | 2 (4.17%) |
| Diabetes complicated with hypertension and gout | 1 (2.08%) |

Residual lesion classification: The residual lesions of COVID-19 patients before discharge (1-2 days) and 14 days after discharge were classified. The percentage of the involvement in each lung lobe was scored as 0 (0%), 1 (1-25%), 2 (26-50%), 3 (51-75%) and 4 (76-100%). The total score of the 5 lung lobes was the total severity score (TSS) of lung inflammation, which was classified as follows: 0 point represents level 0, 1-5 points represent level 1, 6-10 points represent level 2, 11-20 points represent level 3 [8]. Two senior radiologists decided the inflammation level of each patient after consultation.

*Statistical analysis*

All data were recorded in XLSX worksheets and analyzed by IBM SPSS Statistics 25.0 software. Numerical variables were expressed as mean ± standard deviation, median and interquartile range (IQR) values, and comparisons were performed using *t* test and Mann-Whitney U test. Categorical variables were described as percentages (% [n/N]) and were compared using partitions of $\chi^2$ or Fisher test. $P<0.05$ was considered statistically significant.

## Results

*CT findings of patients at different disease stage*

Twenty-eight patients were in early stage (0-4 days after onset of the initial symptom). Among them, 14.29% (4/28) patients had no pulmonary inflammation, 78.57% (22/28) had patchy, segmental ground-glass opacity (GGO) in their lungs and 42.86% (12/28) had interlobular septal thickening. Moreover, 39.29% (11/28) patients developed consolidation and 25.00% (7/28) patients developed "crazy-paving pattern". Typical images are shown in **Figure 1**.

Thirty-nine patients were in progressive stage (5-8 days after the onset of the initial symptom). Among them, 5.13% (2/39) had no lung inflammation, 84.62% (33/39) patients had GGO in their lungs, 53.85% (21/39) patients had interlobular septal thickening in their lungs, and 51.28% (20/39) patients had consolidation in the lungs. Besides, 33.33% (13/39) patients had subpleural curvilinear lines in the lungs, and 28.21% (11/39) had "crazy-paving pattern" and spider web signs. Typical images are shown in **Figure 2**.

Forty-one patients were in peak stage (9-13 days after the onset of the initial symptom). GGO and consolidation were the main manifestations of the lungs at this stage, with incidences of 85.37% (35/41) and 43.9% (18/41). Other chest signs, such as thickening of the pleura, bronchiectasis, and pleural effusion, occurred in 26.83% (11/41), 7.32% (3/41), and 4.89% (2/41) of patients. Typical images are shown in **Figure 3**.

Forty-seven patients were in absorption stage (≥14 days after the onset of the initial symptom). In 38.30% (18/47) patients, lung inflammation disappeared completely. Moreover, compared to other stages, the incidence of GGO, consolidation and "crazy-paving pattern" were significantly reduced by 51.09% (24/47), 2.13% (1/47), and 0.00% (0/47) respectively,

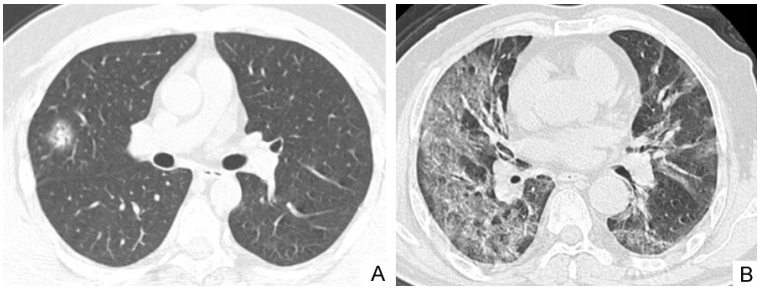

**Figure 1.** CT manifestation of the lung in patients in early stage (0-4 days after onset of the initial symptom). A. Male, 31 years old who underwent CT images on January 28, nodular GGO was seen under the pleura of the upper lobe of the right lung, with high density in the central region. B. Male, 47 years old who underwent CT images on February 4, diffuse GGO was found in both lungs, mainly in the right lung. Some of them were distributed in a fan shape, showing "crazy-paving pattern".

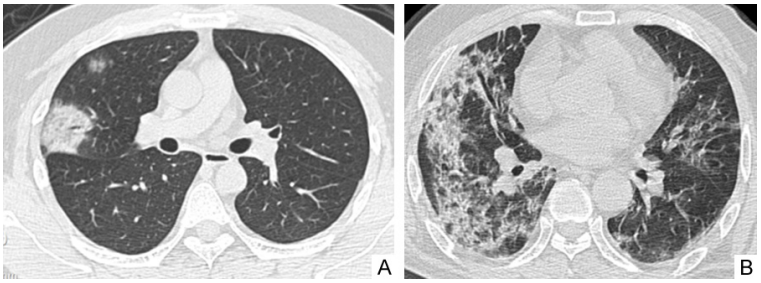

**Figure 2.** CT manifestation of the lung in patients in progressive stage (5-8 days after the onset of the initial symptom). A. Male, 31 years old who underwent CT images on February 1, the lesion range of the upper lobe of the right lung was larger than before, with consolidation and air bronchogram and small patchy GGO. B. Male, 47 years old who underwent CT images on February 11, the right lung lesions were denser than before and mainly distributed under the pleura; the absorption of GGO lesions on the medial side was reduced.

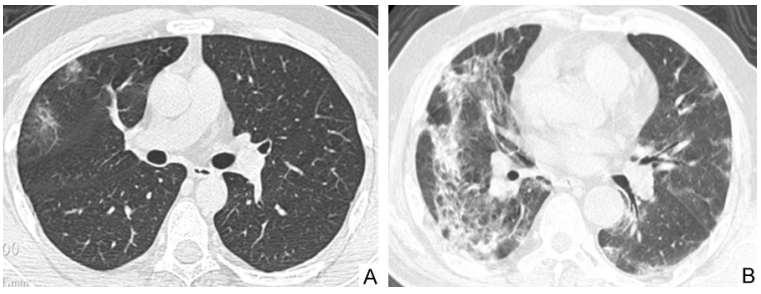

**Figure 3.** CT manifestation of the lung in patients in peak stage (9-13 days after the onset of the initial symptom). A. Male, 31 years old who underwent CT images on February 4, the lesion of the upper lobe of the right lung was obviously absorbed and reduced, and the consolidation shadow basically disappeared, mainly dominated by GGO. B. Male, 47 years old who underwent CT images on February 16, the consolidation and spider web signs were observed, and the pulmonary lesions were reduced.

while the incidence of fibrotic lesions and bronchiectasis significantly increased by 14.89% (7/47), and 10.64% (5/47) respectively. Typical images are shown in **Figure 4**.

The differences in patients with GGO, consolidation, "crazy-paving pattern", subpleural curvilinear line, interlobular septal thickening, pleural thickening, and no pneumonia manifestation by chest HRCT were statistically significant ($P<0.05$) among four different disease periods (early, progressive, peak and resorption stages). However, the differences in patients with fibrotic lesions, spider web sign, bronchiectasis and pleural effusion were not statistically significant ($P>0.05$). As shown in **Table 2**.

*CT findings of patients with different clinical types*

No pneumonia was found on chest CT in one mild patient. Among 38 patients with moderate COVID-19, the main manifestations were GGO (18/38, 47.37%), and GGO with consolidation (16/38, 42.11%), which presented in bilateral lungs (34/38, 89.47%), and multi-lobe distribution (involving 5 lobes) (17/38, 44.74%). Among 9 patients with severe COVID-19, extensive multiple consolidations (3/9, 33.33%) or GGO with consolidation (5/9, 55.56%) in bilateral lungs (9/9, 100.00%), were the main manifestations.

There was a statistically significant difference in GGO between moderate patients and severe patients ($P<0.05$). There was no statistically significant difference in distribution of lesions, consolidation, GGO with consolidation, number of pulmonary lobes involved, lesion size or lesion margin between moderate patients

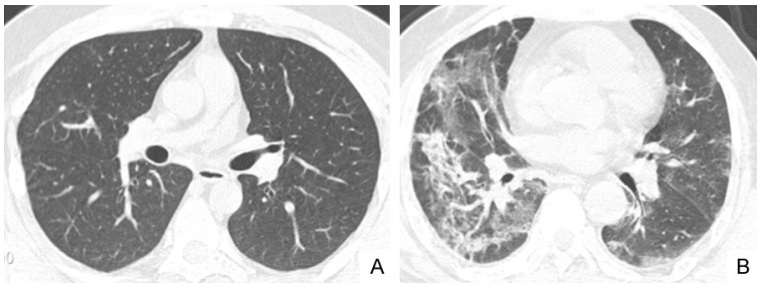


**Figure 4.** CT manifestation of the lung in absorption stage (≥14 days after the onset of the initial symptom). A. Male, 31 years old who underwent CT images on February 26, after three weeks of re-examination, the lesion of the right lung completely disappeared. B. Male, 47 years old who underwent CT images on February 27, the double lung lesions obviously reduced, consolidation basically disappeared, and the residual lesions were mainly GGO and fibrotic lesions.

and severe patients ($P$>0.05), as shown in **Table 3**.

*Comparison of residual lung lesions of patients before and after discharge*

Two weeks after discharge, 28 patients (26 moderate patients and 2 severe patients) returned to the hospital for a review. After discharge, 15 moderate patients (57.69%) had complete absorption of pulmonary inflammation, 1 moderate patient (3.85%) had pulmonary fibrosis, 3 moderate patients (11.54%) had bronchiectasis, 2 moderate patients (7.69%) had pleural thickening, 11 moderate patients (42.31%) and 2 severe patients (100%) still had GGO deformation in the lungs. One severe patient exhibited lung consolidation disappearance.

A total of 26 patients returned to the hospital for CT examinations after 2 weeks of discharge and isolation. The number of patients without pneumonia, the type of lung lesions (GGO, consolidation, spider web sign), inflammatory TSS and classification of residual lesions were compared with the day before discharge, and the differences were statistically significant (all $P$<0.05). There were no statistically significant differences in fibrotic lesions and thickening of the pleura compared with the day before discharge ($P$>0.05), as shown in **Table 4**; **Figure 5**.

## Discussion

*Chest CT features in different stages of disease course*

At the early stage, most of the patients had a patchy and segmental distribution of GGO (22/28, 78.57%), and interstitial changes with interlobular septum thickening (12/28, 42.86%). GGO is a radiological finding in CT consisting of a hazy opacity that is usually caused by protein and fibrous exudation in the alveolar cavity and granulomatous nodules formed by some cellulose, inflammatory cells and multinucleated giant cells. Pulmonary interstitial infiltration signs are related to the diffuse thickening of the alveolar wall, fibrosis and fibroblast proliferation [9]. Study of Guan et al. showed that 56.4% of the 1099 patients showed GGO, which was mostly located under the pleura and the outer middle zone [10]; it might be that the blood flow and lymph in the pulmonary lobules in the subpleural area of the lung periphery are more abundant, so the corresponding inflammatory reaction is more obvious.

At the progressive stage, the number of patients showing consolidation, "crazy-paving pattern" and pulmonary interstitial infiltration signs (such as interlobular septal thickening, subpleural curvilinear line, and spider web sign), as well as the distribution range of lesions increased. This is consistent with the study of Zhou et al., which indicated that as the disease progressed, there were both lung parenchymal and interstitial lesions in the lungs of patients [11]. Moreover, pleural thickening (6/39, 15.38%) and pleural effusion (1/39, 2.56%) were seen in a small number of patients. Consolidation may quickly occur in patients with normal immune function. Histopathologically, consolidation is caused by fibroblast granulation tissue in alveoli, which is related to cell mucous exudate in alveoli [12, 13]. "Crazy-paving pattern" may be caused by alveolar edema and interstitial inflammation during acute lung injury [14]. 2019 nCoV can also lead to diffuse alveolar injury (alveolar edema, hemorrhage), bronchial epithelial exfoliation, cilia loss, squamous metaplasia and hyaline membrane formation [15].

At the peak stage, the number of patients with pulmonary interstitial infiltration and "crazy-paving pattern" decreased. However, GGO (35/41, 85.37%) and consolidation (18/41, 43.90%) were still the main manifestations at

**Table 2.** CT findings of patients with different staging of disease course (n, %)

| Manifestations of chest CT | Early stage (0~4 days) (n=28) | Progressive stage (5~8 days) (n=39) | Peak stage (9~13 days) (n=41) | Absorption stage (≥14 days) (n=47) | *P* value |
|---|---|---|---|---|---|
| GGO | 22 (78.57%) | 33 (84.62%) | 35 (85.37%) | 24 (51.06%) | 0.000 |
| Consolidation | 11 (39.29%) | 20 (51.28%) | 18 (43.90%) | 1 (2.13%) | 0.000 |
| "Crazy-paving pattern" | 7 (25.00%) | 11 (28.21%) | 4 (9.76%) | 0 (0.00%) | 0.000 |
| Fibrotic lesions | 1 (3.57%) | 3 (7.69%) | 5 (12.20%) | 7 (14.89%) | 0.440 |
| Spider web sign | 5 (17.86%) | 11 (28.21%) | 11 (26.83%) | 4 (8.51%) | 0.079 |
| Subpleural curvilinear line | 3 (10.71%) | 13 (33.33%) | 9 (21.95%) | 2 (4.26%) | 0.003 |
| Interlobular septal thickening | 12 (42.86%) | 21 (53.85%) | 12 (29.27%) | 2 (4.26%) | 0.000 |
| Pleural thickening | 0 (0.00%) | 6 (15.38%) | 11 (26.83%) | 7 (14.89%) | 0.014 |
| Bronchiectasis | 1 (3.57%) | 1 (2.56%) | 3 (7.32%) | 5 (10.64%) | 0.522 |
| Pleural effusion | 1 (3.57%) | 1 (2.56%) | 2 (4.89%) | 1 (2.13%) | 0.931 |
| No pneumonia manifestation on HRCT | 4 (14.29%) | 2 (5.13%) | 3 (7.3%) | 18 (38.30%) | 0.000 |

CT, computerized tomography; GGO, ground-glass opacity.

**Table 3.** CT findings of patients with different clinical types (n, %)

| | All (n=47) | Moderate (n=38) | Severe (n=9) | *P* value |
|---|---|---|---|---|
| Distribution of lesions | | | | |
| Left lung | 3 (6.38%) | 3 (7.89%) | 0 (0.00%) | 0.384 |
| Right lung | 1 (2.13%) | 1 (2.63%) | 0 (0.00%) | 0.623 |
| Bilateral lungs | 43 (91.49%) | 34 (89.47%) | 9 (100.00%) | 0.389 |
| Morphology of lesion (Fishe) | | | | |
| GGO | 19 (40.43%) | 18 (47.37%) | 1 (11.11%) | 0.046 |
| Consolidation | 7 (14.89%) | 4 (10.53%) | 3 (33.33%) | 0.084 |
| GGO with consolidation | 21 (44.68%) | 16 (42.11%) | 5 (55.56%) | 0.465 |
| Number of pulmonary lobes involved | | | | 0.319 |
| 1 | 4 (8.51%) | 4 (10.53%) | 0 (0.00%) | |
| 2 | 8 (17.02%) | 7 (18.42%) | 1 (11.11%) | |
| 3 | 4 (8.51%) | 4 (10.53%) | 0 (0.00%) | |
| 4 | 6 (12.77%) | 6 (15.79%) | 0 (0.00%) | |
| 5 | 25 (53.19%) | 17 (44.74%) | 8 (88.89%) | |
| Lesion size | | | | 0.132 |
| < 1 cm | 5 (10.64%) | 5 (13.16%) | 0 (0.00%) | |
| 1-3 cm | 8 (17.02%) | 8 (21.05%) | 0 (0.00%) | |
| >3 cm | 34 (72.34%) | 25 (65.79%) | 9 (100.00%) | |
| Lesion margin | | | | 0.410 |
| Clear | 13 (27.66%) | 12 (31.58%) | 1 (11.11%) | |
| Vague | 34 (72.34%) | 26 (68.42%) | 8 (88.89%) | |

CT, computerized tomography; GGO, ground-glass opacity.

this stage. The number of patients of other chest signs such as pleural thickening (11/41, 26.83%) and pleural effusion (2/41, 4.89%) increased. According to the previous experience of MERS-CoV and H5N1 avian influenza virus infection, the presence of pleural effusion may indicate poor prognosis of COVID-19 [16].

Finally, at the absorption stage, lung inflammation completely disappeared in 38.30% of patients, and the number of patients with GGO, consolidation, crazy-paving pattern, and pulmonary interstitial infiltration signs (spider web sign, subpleural curvilinear line, interlobular septal thickening) was significantly reduced

**Table 4.** Comparison of residual lung lesions of patients before and after discharge (n, %)

| | One day before discharge | | | >14 days after discharge | | | $P^a$ value | $P^b$ value |
|---|---|---|---|---|---|---|---|---|
| | All (n=28) | Moderate (n=26) | Severe (n=2) | All (n=28) | Moderate (n=26) | Severe (n=2) | | |
| Lesion type | | | | | | | | |
| No pneumonia manifestation on lungs | 2 (7.14%) | 2 (7.69%) | 0 (0.00%) | 15 (53.57%) | 15 (57.69%) | 0 (0.00%) | 0.000 | 0.000 |
| GGO | 25 (89.29%) | 23 (88.46%) | 2 (100.00%) | 13 (46.43%) | 11 (42.31%) | 2 (100.00%) | 0.000 | 0.001 |
| Consolidation | 6 (21.43%) | 5 (19.23%) | 1 (50.00%) | 0 (0.00%) | 0 (0.00%) | 0 (0.00%) | 0.000 | 0.023 |
| Fibrotic lesions | 0 (0.00%) | 0 (0.00%) | 0 (0.00%) | 1 (3.57%) | 1 (3.85%) | 0 (0.00%) | 0.312 | 0.312 |
| Bronchiectasis | 3 (10.71%) | 3 (11.54%) | 0 (0.00%) | 3 (10.71%) | 3 (11.54%) | 0 (0.00%) | 1 | 1 |
| Pleural thickening | 3 (10.71%) | 3 (11.54%) | 0 (0.00%) | 2 (7.14%) | 2 (7.69%) | 0 (0.00%) | 0.638 | 0.638 |
| Spider web sign | 4 (14.29%) | 4 (15.38%) | 0 (0.00%) | 0 (0.00%) | 0 (0.00%) | 0 (0.00%) | 0.038 | 0.038 |
| TSS of lung inflammation | 5.04±4.33 | 4.42±3.80 | 13.00±2.83 | 2.39±3.57 | 1.88±2.96 | 9.00±5.66 | 0.010 | 0.016 |
| Residual lesion classification | | | | | | | 0.001 | 0.001 |
| Level 0 | 2 (7.14%) | 2 (7.69%) | 0 (0.00%) | 15 (53.57%) | 15 (57.69%) | 0 (0.00%) | | |
| Level 1 (1-5) | 14 (50.00%) | 14 (53.85%) | 0 (0.00%) | 9 (32.14%) | 8 (30.77%) | 1 (50.00%) | | |
| Level 2 (6-10) | 8 (28.57%) | 8 (30.77%) | 0 (0.00%) | 3 (10.71%) | 3 (11.54%) | 0 (0.00%) | | |
| Level 3 (>10) | 4 (14.29%) | 2 (7.69%) | 2 (100.00%) | 1 (3.57%) | 0 (0.00%) | 1 (50.00%) | | |

Note: $P^a$: comparison of moderate type before and after discharge. $P^b$: comparison of the total number of items before discharge and the total number of items after discharge. GGO, ground-glass opacity; TSS, total severity score.

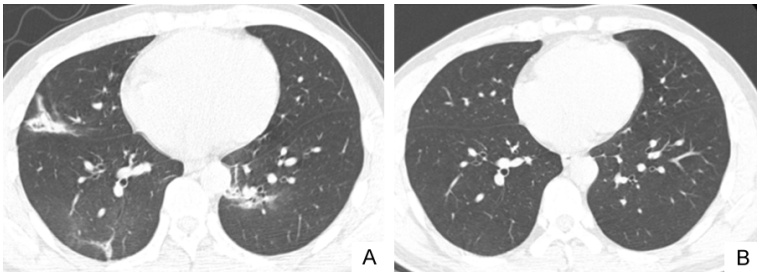


**Figure 5.** CT manifestation of the lung in typical patients. Male, 30 years old with CT re-examination (A) before (February 3) and (B) after discharge (February 27). (A) Striped high-density shadow and thin flaky GGO were seen in the middle lobe of the right lung and the lower lobe of both lungs. A striped shadow was seen in the lower lobe of the right lung near the pleura. (B) The lung lesions were basically absorbed.

compared with a peak stage. However, the number of patients with pulmonary fibrosis and bronchiectasis increased. Signs of paving disorder or grid-like changes may be lymphatic tract involvement or interstitial pulmonary edema. The pathological changes of the patient are basically consistent with the dynamic process of CT. Wang et al. also pointed out that the time changes of different CT manifestations have a certain regularity, suggesting the progression and recovery of the disease [17].

After discharge, 28 patients returned to the hospital for a review. In 13 moderate patients, newly-increased lung lesions were completely absorbed, and the lung consolidation in all other patients basically disappeared; yet, GGO distribution was still the main feature. Re-examination of 2 severe patients showed that the lung lesions were reduced, and only GGO remained.

*Chest CT features in different clinical classifications*

Pulmonary HRCT showed no pneumonia manifestation in 1 mild patient (**Figure 6**). Among the moderate patients, 4 cases had negative chest HRCT in the early stage of the disease course, and GGO in patches, nodules or lobes began to appear in the lungs in the progressive stage. Lesions of a total of 89.47% of the moderate patients were distributed in both lungs. They were mainly with GGO or GGO with consolidation shadow, involving 5 lung segments (17/38, 44.74%), blurred lesion margin (26/38, 68.42%), and the lesion diameter larger than 3 cm (25/38, 65.79%). There were 3 severe patients (3/9, 33.33%) dominated by consolidation and 5 patients (5/9, 55.56%) showed GGO with consolidation; among them, the occupation involved 5 lung lobes (8/9, 88.89%), blurred edges (8/9, 88.89%), and the lesion range larger than 3 cm (9/9, 100%). Thoracic residual lesions in severe patients were mainly distributed in the form of GGO, including 1 patient with reticular shadow and pleural thickening. It is suggested that as the condition of

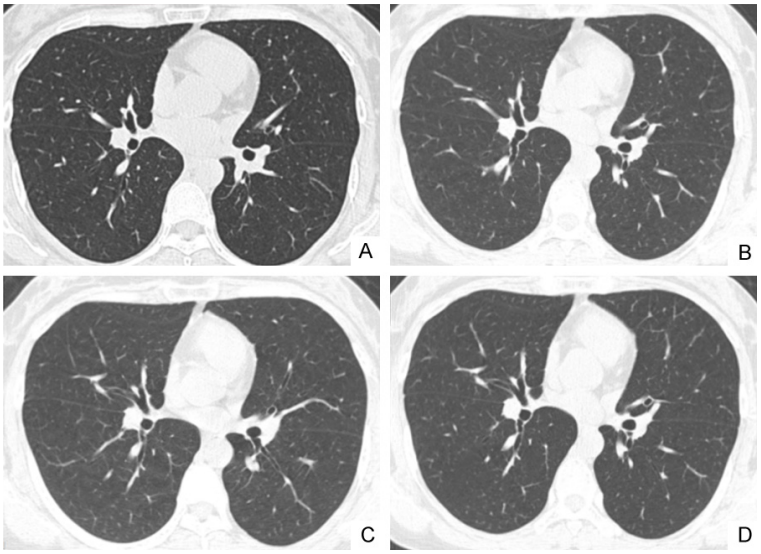


**Figure 6.** CT manifestation of the lung in a mild patient at different stages of disease course. Female, 38 years old who underwent CT on February 13 (A), February 17 (B), February 21 (C), and February 27 (D), respectively. No pneumonia manifestation was found in the lung at different stages.

COVID-19 patients gets worse, the larger area of the lung tissue is involved and the distribution is wider, which conforms to the dynamic changes of COVID-19. CT imaging features can be used as an effective supplement to determine whether COVID-19 patients are severe or critical in clinical diagnosis and treatment programs [8].

*COVID-19 differential diagnosis*

The chest CT of patients with COVID-19 needs to be distinguished from other types of viral pneumonia, such as influenza A (H1N1), H7N9 avian influenza virus and adenovirus.

*Influenza A (H1N1) viral pneumonia*

H1N1 influenza is more prevalent in young people, obese patients and pregnant women [18]. The moderate manifestations of H1N1 influenza include lobular central nodules, ground-glass-like degeneration (diffuse or lobular distribution), segmental consolidation, and bronchiectasis caused by bronchioles. According to a previous study, a total of 89% of patients had 3 or more lung segment abnormalities, accompanied by a small amount of unilateral or bilateral pleural effusion. Patients with pleural effusion and consolidation showed poor prognosis [19].

*Human infection with H7N9 avian influenza virus inflammation*

Acute respiratory symptoms are the main character of H7N9 avian influenza virus infection, and the disease progresses rapidly. Lesions mostly occur in a single lobe, mainly on the dorsal side of the lower lobe, and the early stage of disease course is dominated by GGO. With the aggravation of the disease, the lesions gradually consolidate and can be seen with interlobular septal thickening and air bronchogram [20]. Pleural effusion tends to occur in most patients (88.9%). During the follow-up of H7N9 patients, pulmonary fibrosis was more moderate. Patients with acute respiratory distress syndrome were more serious than H1N1 and had a poor prognosis [21].

*Adenovirus pneumonia*

Human adenovirus is a non-enveloped double-stranded DNA virus, with more than 50 serotypes [22]. Adenovirus pneumonia mainly occurs in winter and spring, and its clinical manifestations include pharyngitis, bronchiolitis or bronchopneumonia [23]. In most of older patients with immune deficiency and chronic underlying diseases, respiratory failure, disseminated infection, hemorrhagic cystitis and even death may occur. Adenoviruses mainly involve peripheral bronchioles, causing bronchiolitis, which may be accompanied by necrotizing bronchopneumonia. Chest CT shows diffuse or localized GGO of both lungs or lobular or segmental distribution of bronchopneumonia. Excessive inflation and lobar atelectasis tend to be moderate in infants and children [24].

There are still some limitations in this study. First, the sample size was relatively small. Moreover, there is a lack of relevant clinical diagnosis, treatment and imaging data for critically ill patients. As some patients were treated in other places, their imaging data were not complete, and they were not sure about their

exact date of disease onset (such as recall deviation), which could have a certain impact on our evaluation. In addition, COVID-19 and other viral pneumonia have some overlapping imaging manifestations [25].

## Conclusion

CT examination is the main method for diagnosing novel coronavirus pneumonia. It can detect lesions in the early stage, observe the scope of lesions, evaluate the severity of lesions, understand the imaging manifestations of novel coronavirus pneumonia in various stages, and dynamically detect the changes of disease conditions. It is of great value for the diagnosis, treatment and prognosis of diseases. In particular, it has a significant role in the formulation of discharge standards. Early detection of asymptomatic patients has an important role in timely laboratory examination and early isolation, avoidance of contact infection, and prevention and control of the pandemic. Therefore, chest CT scanning is of great significance for the treatment of patients and the prevention and control of the pandemic.

## Acknowledgements

This study was supported by the Hengyang Science and Technology Plan Project-Basic Research Project of Prevention and Treatment of the Novel Coronavirus Pneumonia (No. 202010031577), the Novel Coronavirus Pneumonia Emergency Project of the University of South China (No. 2020-15 and No. 2020-25), the Scientific Research Project of Hunan Provincial Health and Family Planning Commission (No. A2017015), the National Natural Science Foundation of China (No. 81373465), the Provincial and Municipal Joint Foundation of Natural Science of Hunan Province, China (No. 2016JJ5010), and the Science and Technology Innovation Program of Hunan Province (2018SK51712).

## Disclosure of conflict of interest

None.

## Abbreviations

2019 nCoV, coronavirus 2019; COVID-19, Corona Virus Disease 2019; CT, computerized tomography; GGO, ground-glass opacity.

**Address correspondence to:** Ting Xie, Department of Nephrology, The Affiliated Nanhua Hospital, Hengyang Medical College, University of South China, No. 336 Dongfeng South Road, Zhuhui District, Hengyang 421002, Hunan, China. Tel: +86-15211850046; E-mail: 1023561022@qq.com; Xuefeng Yang, Department of Gastroenterology and General Practice, The Affiliated Nanhua Hospital, Hengyang Medical College, University of South China, No. 336 Dongfeng South Road, Zhuhui District, Hengyang 421002, Hunan, China. Tel: +86-18973405898; E-mail: yxf9988@126.com

## References

[1] Jin YH, Cai L, Cheng ZS, Cheng H, Deng T, Fan YP, Fang C, Huang D, Huang LQ, Huang Q, Han Y, Hu B, Hu F, Li BH, Li YR, Liang K, Lin LK, Luo LS, Ma J, Ma LL, Peng ZY, Pan YB, Pan ZY, Ren XQ, Sun HM, Wang Y, Wang YY, Weng H, Wei CJ, Wu DF, Xia J, Xiong Y, Xu HB, Yao XM, Yuan YF, Ye TS, Zhang XC, Zhang YW, Zhang YG, Zhang HM, Zhao Y, Zhao MJ, Zi H, Zeng XT, Wang YY and Wang XH. A rapid advice guideline for the diagnosis and treatment of 2019 novel coronavirus (2019-nCoV) infected pneumonia (standard version). Mil Med Res 2020; 7: 4.

[2] Xiong Y, Sun D, Liu Y, Fan Y, Zhao L, Li X and Zhu W. Clinical and high-resolution CT features of the COVID-19 infection: comparison of the initial and follow-up changes. Invest Radiol 2020; 55: 332-339.

[3] Tavare AN, Braddy A, Brill S, Jarvis H, Sivaramakrishnan A, Barnett J, Creer DD and Hare SS. Managing high clinical suspicion COVID-19 inpatients with negative RT-PCR: a pragmatic and limited role for thoracic C. Thorax 2020; 75: 537-538.

[4] Zhong ZF, Huang J, Yang X, Peng JL, Zhang XY, Hu Y, Fu N, Lin HL, Jiang B, Tian YY, Yao HY, Deng LP, Tang XQ, Zhou JC, Tang J, Xie X, Liu Q, Liu J, Dou CY, Dai RJ, Yan B and Yang XF. Epidemiological and clinical characteristics of COVID-19 patients in Hengyang, Hunan Province, China. World J Clin Cases 2020; 8: 2554-2565.

[5] Xie X, Zhong Z, Zhao W, Zheng C, Wang F and Liu J. Chest CT for typical coronavirus disease 2019 (COVID-19) pneumonia: relationship to negative RT-PCR testing. Radiology 2020; 29: 41-45.

[6] National Health Commission and State Administration of Traditional Chinese Medicine. New Coronavirus Pneumonia Diagnosis and Treatment Plan (Trial Version 7). Jiangsu Journal of Traditional Chinese Medicine 2020; 52: 1-6.

[7] Infectious Disease Group Radiology Branch of Chinese Medical Association, Infectious Imag-

ing Committee of Radiologist Branch of Chinese Medical Doctor Association, Infection and Inflammation Radiology Branch of Chinese Research Hospital Association, Infection (Infectious Disease) Imaging Working Committee of Chinese Association for STD and AIDS Prevention and Treatment, China Infectious Disease Imaging Group of Infectious Disease Branch of Hospital Association, Infectious Disease Group of General Radiological Equipment Professional Committee of China Equipment Association and Beijing Imaging Diagnosis and Treatment Technology Innovation Alliance. Guideline for imaging diagnosis of novel coronavirus (2019-nCoV) infected pneumonia (1st edition 2020). New Medicine 2020; 30: 22-34.

[8] Li K, Fang Y, Li W, Pan C, Qin P, Zhong Y, Liu X, Huang M, Liao Y and Li S. CT image visual quantitative evaluation and clinical classification of coronavirus disease (COVID-19). Eur Radiol 2020; 30: 4407-4416.

[9] Tian S, Hu W, Niu L, Liu H, Xu H and Xiao SY. Pulmonary pathology of early-phase 2019 novel coronavirus (COVID-19) pneumonia in two patients with lung cancer. J Thorac Oncol 2020; 15: 700-704.

[10] Guan WJ, Ni ZY, Hu Y, Liang WH, Ou CQ, He JX, Liu L, Shan H, Lei CL, Hui DSC, Du B, Li LJ, Zeng G, Yuen KY, Chen RC, Tang CL, Wang T, Chen PY, Xiang J, Li SY, Wang JL, Liang ZJ, Peng YX, Wei L, Liu Y, Hu YH, Peng P, Wang JM, Liu JY, Chen Z, Li G, Zheng ZJ, Qiu SQ, Luo J, Ye CJ, Zhu SY and Zhong NS. Clinical characteristics of coronavirus disease 2019 in China. N Engl J Med 2020; 382: 1708-1720.

[11] Zhou S, Wang Y, Zhu T and Xia L. CT features of coronavirus disease 2019 (COVID-19) pneumonia in 62 patients in Wuhan, China. AJR Am J Roentgenol 2020; 214: 1287-1294.

[12] Zare MM, Kahkouee S and Pourabdollah M. Radio-pathological correlation of organizing pneumonia (OP): a pictorial review. Br J Radiol 2017; 90: 20160723.

[13] Xu Z, Shi L, Wang Y, Zhang J, Huang L, Zhang C, Liu S, Zhao P, Liu H, Zhu L, Tai Y, Bai C, Gao T, Song J, Xia P, Dong J, Zhao J and Wang FS. Pathological findings of COVID-19 associated with acute respiratory distress syndrome. Lancet Respir Med 2020; 8: 420-422.

[14] Wu J, Wu X, Zeng W, Guo D, Fang Z, Chen L, Huang H and Li C. Chest CT findings in patients with coronavirus disease 2019 and its relationship with clinical feature. Invest Radiol 2020; 55: 257-261.

[15] Nicholls JM, Poon LL, Lee KC, Ng WF, Lai ST, Leung CY, Chu CM, Hui PK, Mak KL, Lim W, Yan KW, Chan KH, Tsang NC, Guan Y, Yuen KY and Peiris JS. Lung pathology of fatal severe acute respiratory syndrome. Lancet 2003; 361: 1773-1778.

[16] Shi H, Han X, Jiang N, Cao Y, Alwalid O, Gu J, Fan Y and Zheng C. Radiological findings from 81 patients with COVID-19 pneumonia in Wuhan, China: a descriptive study. Lancet Infect Dis 2020; 20: 425-434.

[17] Wang Y, Dong C, Hu Y, Li C, Ren Q, Zhang X, Shi H and Zhou M. Temporal changes of CT findings in 90 patients with COVID-19 pneumonia: a longitudinal study. Radiology 2020; 296: 55-64.

[18] Rohani P, Jude CM, Chan K, Barot N and Kamangar N. Chest radiological findings of patients with severe H1N1 pneumonia requiring intensive care. J Intensive Care Med 2016; 31: 51-60.

[19] Schoen K, Horvat N, Guerreiro NFC, de Castro I and de Giassi KS. Spectrum of clinical and radiographic findings in patients with diagnosis of H1N1 and correlation with clinical severity. BMC Infect Dis 2019; 19: 964.

[20] Dai J, Zhou X, Dong D, Liu Y, Gu Q, Zhu B, Wu C and Cai H. Human infection with a novel avian-origin influenza A (H7N9) virus: serial chest radiographic and CT findings. Chin Med J (Engl) 2014; 127: 2206-2211.

[21] Li H, Weng H, Lan C, Zhang H, Wang X, Pan J, Chen L and Huang J. Comparison of patients with avian influenza A (H7N9) and influenza A (H1N1) complicated by acute respiratory distress syndrome. Medicine (Baltimore) 2018; 97: 194.

[22] Buckwalter SP, Teo R, Espy MJ, Sloan LM, Smith TF and Pritt BS. Real-time qualitative PCR for 57 human adenovirus types from multiple specimen sources. J Clin Microbiol 2012; 50: 766-771.

[23] Yoon H, Jhun BW, Kim SJ and Kim K. Clinical characteristics and factors predicting respiratory failure in adenovirus pneumonia. Respirology 2016; 21: 1243-1250.

[24] Koo HJ, Lim S, Choe J, Choi SH, Sung H and Do KH. Radiographic and CT features of viral pneumonia. Radiographics 2018; 38: 719-739.

[25] Chen L, Liu HG, Liu W, Liu J, Liu K, Shang J, Deng Y and Wei S. Analysis of clinical features of 29 patients with 2019 novel coronavirus pneumonia. Zhonghua Jie He He Hu Xi Za Zhi 2020; 43: 203-208.